CONSTRUCTION
e-ISSN: 2785-8731
VOL. 2, ISSUE 1, 103 – 117
DOI: https://doi.org/10.15282/cons.v2i1.7428

ORIGINAL ARTICLE

Thailand Country Research 2021 on Wind Engineering Activities

V. Boonyapinyo[1,*] and J. Junruang[2]

[1]Thammasat School of Engineering, Thammasat University, Rangsit Campus, Pathumthani 12120, Thailand.
[2]Rajamangala University of Technology Tawan-ok, Uthenthawai Campus, Bangkok 10330, Thailand.

ABSTRACT – In this paper, Thailand Country Research 2021 on Wind Engineering Activities is present. Firstly, development of DPT Standard 1311-50 for wind loading calculation and response of buildings in Thailand is present. The DPT Standard is financially supported by Department of Public Works and Town & Country Planning. The new standard is more accurate than the building code No.6 because it considers the wind speed zoning, surrounding terrain, building shapes, and dynamic properties. Secondly, wind engineering activities by subcomitted on wind and earthquake effects, Engineering Institute of Thailand and subcomitted on coordinations for disasters and public safety, Council of Engineers Thailand are present. Finally, research examples of wind load studies of bridges and buildings by TU-AIT wind tunnel test are also presented. The two parallel configurations of the bridge result in vortex-induced vibrations (VIV) and significantly lower the flutter speed compared with the new bridge alone. The new bridge also results in significant reduction of the flutter speed of downstream existing bridge.

ARTICLE HISTORY
Received: 06th Feb 2022
Revised: 29th Mar 2022
Accepted: 23th Apr 2022

KEYWORDS
Wind Loading Standard
DPT standard 1311-50
Wind Tunnel Tes
High-Rise Buildings
Two Parallel Long-Span Bridges

INTRODUCTION

Although typhoon represents rare incident, Thailand experienced a number of wind disasters from several tropical storms and one typhoon in the past 59 year's history (1951-2009). After the devastating cyclone and storm surge occurred in Myanmar in May 2008, wind-related disaster risk reduction activities in Thailand become increasingly interesting. In this paper, Thailand Country Report 2021 on Wind Engineering Activities is present. Firstly, development of DPT Standard 1311-50 for wind loading calculation and response of buildings in Thailand is present. Secondly, wind engineering activities by subcomitted on wind and earthquake effects, Engineering Institute of Thailand and subcomitted on coordinations for disasters and public safety, Council of Engineers Thailand are present. Finally, research examples of wind load studies of bridges and buildings by TU-AIT wind tunnel test are also presented

DEVELOPMENT OF DPT STANDARD 1311-50 FOR WIND LOAD CALCULATION AND RESPONSE OF BUILDINGS

The wind load specified in the existing building code under the Building Control Act (BCA) 1979 is obsolete because it does not consider the terrain conditions and the typhoon influence and then the wind pressures depend on only the height and apply the same value for whole country. In addition, the code value is too low for very tall building, and for building in open exposure, as well as buildings in the Southern part of Thailand which is prone to typhoon attack [1, 2]. Therefore, the subcommittee on wind and earthquake effects on structures of the Engineering Institute of Thailand published the wind loading standard for building design in 2003 [3]. It considers the wind speed zoning, surrounding terrain, dynamic properties, and building shapes. The standard is mainly based on the National Building Code of Canada 1995 [4].

However, the wind loading standard for building design in 2003 has been revised again for up-to-date wind loading standard. At present, DPT standard 1311-50 (Fig. 1) for wind loading calculation and response of buildings in Thailand is newly published by Department of Public Works and Town & Country Planning [5-6]. To develop the new wind loading standard for building design, an evaluation and comparison of wind load and responses for building among several codes/standards, and wind tunnel test for pressure measurement and overall wind load were studied by Boonyapinyo et al. [5], among others. The new development of DPT standard 1311-50 [6] is mainly based on NBCC-2005 [7], partly on AIJ-2004 [8] for across-wind and torsional load and response, and partly on ASCE7-05 [9] for wind load combination for rigid structures and ideal of wind load for low-rise building in table. The new development of DPT standard 1311-50 for wind loading calculation and response of buildings over 2003 version includes the specified wind load and response, reference wind speed map, natural frequency and damping of building, table for design wind loads for main structures, secondary members and claddings for low-rise buildings, wind tunnel test procedure, commentary, numerical examples, computer program for calculation of wind load and response, and wind load on miscellaneous structures such as, large billboards, cylinders, poles, structural member, two- and three-dimensional trusses. The reference wind speed is based on the study of the wind climate in Thailand [5]. The wind speed for the Southern Thailand reflects the influence of the rare event of the typhoons in the region. The natural frequency and damping for building in Thailand are based on the measurements of 50 buildings in Bangkok.

*CORRESPONDING AUTHOR | V. Boonyapinyo | ✉ bvirote@engr.tu.ac.th

Wind load calculation procedure

Three different approaches for determining design wind loads on buildings and structures are given in the standard as follows.

(a) Simple procedure: The simple procedure is appropriate for use with the majority of wind loading applications, including the structure and cladding of low and medium rise building and the cladding design of high rise buildings. These are situations where the structure is relatively rigid. Thus, dynamic actions of the wind do not require detailed knowledge of the dynamic properties of the buildings and can be dealt with by equivalent static loads.

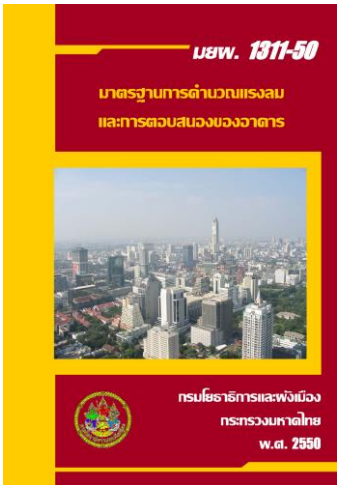

Figure 1. DPT standard 1311-50 [5, 6]

Figure 2. Example of model in boundary-layer Long-wind tunnel of TU-AIT.

(b) Detailed procedure: The detailed procedure is appropriated for buildings whose height is greater than 4 times their minimum effective width or greater than 80 m and other buildings whose light weight, low frequency and low damping properties make them susceptible to vibration.

(c) Wind tunnel test procedure: Wind tunnel testing is appropriate when more exact definition of dynamic response is needed and for determining exterior pressure coefficients for cladding design on buildings whose geometry deviates markedly from more common shapes for which information is already available. Detail of wind tunnel test procedure is given in [5-6]. Figure 2 shows the boundary-layer long-wind tunnel that was jointly built by Thammasat university (TU) and Asian Institute of Technology (AIT) at Thammasat University. The test section is 2.5x2.5 m with 25.5 m in length. Wind speed is in the range of 0.5 to 20 m/s.

Specified external pressure or suction

The specified external pressure or suction due to wind on part or all of a surface of a building shall be calculated from

$$p = I_w q C_e C_g C_p \tag{1}$$

where; p = the specified external pressure acting statically and, in a direction, normal to the surface either as a pressure directed towards the surface or as a suction directed away from the surface, I_w = importance factor for wind load, as provided in Table 1, q = the reference velocity pressure, C_e = the exposure factor, C_g = the gust effect factor, C_P = the external pressure coefficient, averaged over the area of the surface considered

The net wind load for the building as a whole shall be the algebraic difference of the loads on the windward and the leeward surfaces, and in some cases may be calculated as the sum of the products of the external pressures or suctions and the areas of the surfaces over which they are averaged

Reference velocity pressure

The reference wind pressure, q, is determined from reference (or design) wind speed, $\overline{V}$ by the following equation

$$q(\text{in kg/m}^2) = \frac{1}{2}\left(\frac{\rho}{g}\right)\overline{V}^2 \tag{2}$$

where; ρ = air density = 1.25 kg/m^3, g = acceleration due to gravity = 9.81 m/s^2, $\overline{V}$ = design wind speed, $\overline{V} = V_{50}$ for serviceability limit state, $\overline{V} = T_F \cdot V_{50}$ for ultimate (strength) limit state, V_{50} = reference wind speed that is based on one-

hour average wind speed at 10 m. in open terrain in 50-years return period. V_{50} and typhoon factor (T_F) are shown in Table 1 and Figure 3.

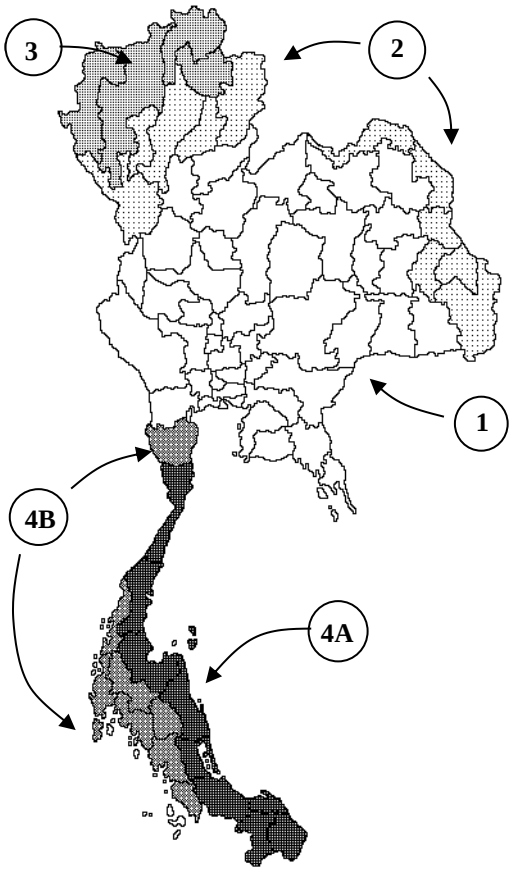

Figure 3. DPT standard 1311-50 [5, 6].

Table 1. Reference wind speeds and typhoon factor.

Zone	Area	V_{50}	T_F
Zone 1	Central region	25	1.0
Zone 2	Lower part of Northern region and East west border region	27	1.0
Zone 3	Upper part of Northern region	29	1.0
Zone 4 A	East coast of Southern peninsula	25	1.2
Zone 4 B	Petchaburi and West coast of Southern peninsula	25	1.08

WIND ENGINEERING ACTIVITIES

Subcomitted on wind and earthquake effects, Engineering Institute of Thailand

To encourage the engineers using the wind load standard, subcomitted on wind and earthquake effects, Engineering Institute of Thailand will hold the seminar on wind effects on structures and wind load calculation for building design by DPT standard 1311-50 on 24 – 26 Novenber 2021 and 8 – 10 June 2022.

Subcomitted on coordinations for disasters and public safety, Council of Engineers Thailand

In Thailand, Thunderstorm have caused severe damage to buildings, structures, crops, etc. Lessons learned from Thunderstorm and other can greatly contribute to countermeasure against future natural calamities. Subcomitted on coordinations for disasters and public safety, Council of Engineers Thailand held the seminar on Natural disaster from Thunderstorm and engineering preparation on 25 August, 2020 and the seminar on Lessons learned from Thunderstorm on 2 September, 2021.

(a) The original stand-alone configuration (b) Image of the new bridge (behind) with the existing bridge (front)

Figure 4. The Rama IX bridge in Thailand.

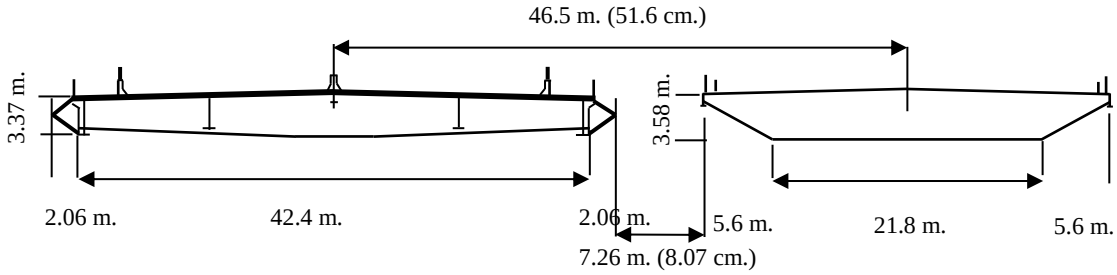

(a) New bridge (b) Existing bridge

Figure 5. Cross section of prototype and position of two parallel bridge deck sections (Dimension for the scaled model are shown in parentheses).

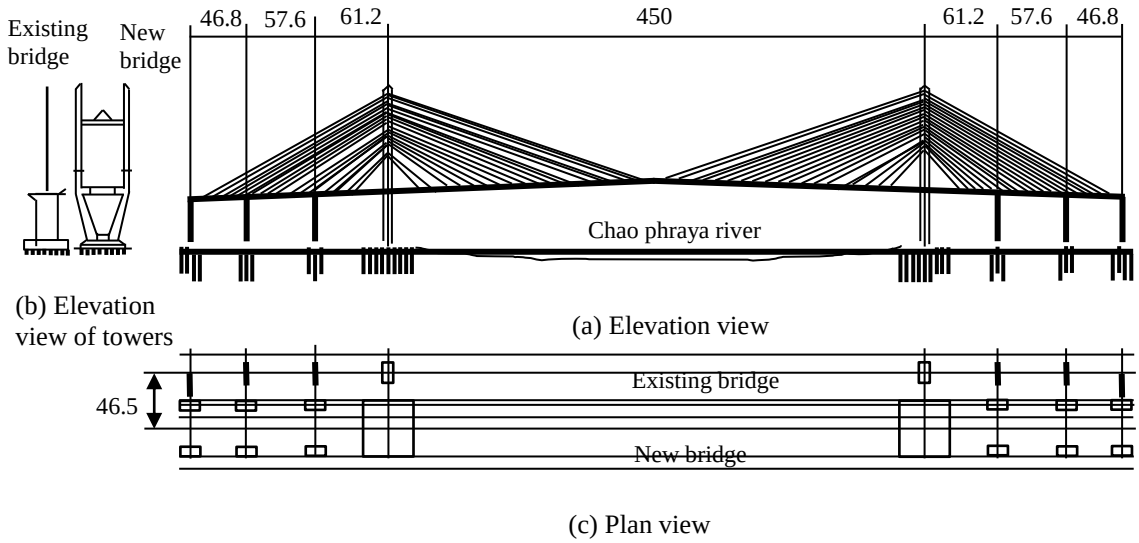

Figure 6. Layout of the existing and the new Rama IX bridge (unit: m.).

RESEARCH ON VORTEX INDUCED VIBRATION AND FLUTTER INSTABILITY OF TWO PARALLEL CABLE-STAYED BRIDGES

Description of the two parallel cacle-stayed bridge

The existing Rama IX bridge (see Fig. 4a) carries six lanes of expressway traffic across the Chao Phraya River in Bangkok, Thailand. It connected the Yan Nawa District to Rat Burana District as a part of the Dao Khanong - Port Section of Chalerm Maha Nakhon Expressway. The bridge opened to traffic in 1987, with a 450 m long cable-stayed section over the river and two 166-meter side spans. The deck is a steel box girder with orthotropic deck and steel pylons are supported on concrete piers and pile foundations.

Table 2. Dynamic parameters for the sectional model.

Parameters	Similarity scale	New Rama IX bridge		Existing Rama IX bridge	
		Prototype	Model	Prototype	Model
Length (m.)	λ_L	-	2.26	-	2.26
Width (m.)	λ_L	42.4	0.471	33	0.367
Height (m.)	λ_L	3.87	0.043	4	0.045
Mass (kg/m.)	λ_L^2	58,486	7.05	25,467	3.10
Mass moment of inertia (kg m^2/m)	λ_L^4	7,571,830	0.1123	2,010,000	0.0309
First vertical frequency (Hz.)	λ_f	0.291	2.132	0.32	2.322
First torsional frequency (Hz.)	λ_f	0.416	3.034	0.67	4.903
Torsional to vertical frequency ratio	1	1.43	1.42	2.09	2.11
Vertical damping ratio (%)	1	0.40	0.25	0.40	0.45
Torsional damping ratio (%)	1	0.25	0.14	0.25	0.31

The Expressway and Rapid Transit Authority of Thailand (ETA) plan to build a new bridge which parallel to the old bridge (see Fig. 4b). The new Rama ix bridge carries eight lanes of expressway and constructed to solve traffic congestion from Thonburi side to the city of Bangkok. The new bridge is a cable-stayed bridge, with two longitudinal steel box girders connected by transverse steel cross beam spread evenly along the bridge. The dimensions of the two decks are shown in Fig. 5 and the layout of the existing Bridge and the new Rama IX Bridge are shown in Fig. 6.

The targets of the wind tunnel experimental were to assess the interference of the existing bridge on the new bridge, and via versus in terms of effects on aerodynamic coefficients, vortex-induced vibrations, flutter instability and flutter derivative.

Wind tunnels tests

In order to study the interferences effect of two parallel decks on aerodynamic static and aeroelastic, the test of two-edge girder type blunt section models (see Fig. 7) were performed in TU-AIT boundary layer wind tunnel in Thammasat University, Thailand. The working section of wind tunnel has a width of 2.5 m, a height of 2.5 m., a length of 25.5 m. and wind speed is in the range of 0.5 to 20 m/s. A 1:90 geometrically scaled section models of the two bridges were constructed by aluminum and acrylic. The length of the section model was selected as 2.26 m to be compatible with the wind tunnel used. All details were scaled down geometrically, with exception of some details such as railings that use equivalent area. Dynamic properties of the existing Rama IX cable-stayed bridges were obtained from the Rama IX Bridge Tenth-Year [10]. In addition, the main span of new bridge has the same length of existing bridge (450 m.) but the deck width is 42.4 m (see Fig. 5 and 6). The gap distance between two bridges is 7.26 m. Dynamic properties of the new Rama IX cable-stayed bridges were obtained from the Epsilon Co. Ltd. and Weicon Co. Ltd. [11]. Table 2 list the main parameters of the actual bridge and the section model of the new and existing bridge, respectively. The length scale λ_L = 1:90, frequency scale λ_f = 7.32, velocity scale λ_V = 12.28 and modal damping ξ_h = 0.23%, ξ_α = 0.14% for new bridge. The length scale λ_L = 1:90, frequency scale λ_f = 7.25, velocity scale λ_V = 12.40 and modal damping ξ_h = 0.45%, ξ_α = 0.31% for existing bridge.

Interferences effects of two-parallel bridge decks on vortex-induced vibration and flutter response

According to the wind-resistant design manual for highway bridges in Japan (Sato, 2003), the allowable amplitudes of new bridge for vertical bending were ((0.04/0.291)*100) = 13.75 cm. in term of maximum vertical displacement, which is equivalent to 9.8 cm. in term of RMS vertical displacement and (2.28/(15.22*0.416)) = 0.36° in term of maximum torsional degree, which is equivalent to 0.25° in term of RMS torsional degree.

For existing bridge, the allowable amplitudes of vertical bending were ((0.04/0.32)*100) = 12.5 cm. in term of maximum vertical displacement, which is equivalent to 8.9 cm. in term of RMS vertical displacement and (2.28/(13.54*0.67)) = 0.25° in term of maximum torsional degree, which is equivalent to 0.17° in term of RMS torsional degree.

It should be note that this research was emphasized on the sectional model test of two parallel bridges. The maximal VIV responses of the full bridge are different from VIV responses directly obtained via sectional model. A modal shape effect and spanwise correlation of the fluctuating wind which can be obtained based on proper model of vortex-induced force. These effects should be considered in further work when transforming the VIV responses of the sectional model to those of the full bridge.

From the sectional bridge model test in wind tunnel, the new bridge alone (case 1) with fairing and damping ratio (ξ_h = 0.23% for heave and ξ_a = 0.14% for pitching) and the existing bridge alone with damping ratio (ξ_h = 0.45% for heave and ξ_a = 0.31% for pitching) show no problem in vortex-induced vibration. These results agree well with the similar, previous research by Boonyapinyo et al. [12] who investigated the effects of fairing modification on VIV and flutter instability of the Industrial Ring Road Bridge (the Bhumibol Bridge) in Thailand by section model test. Those results shown that the modified section with fairing can suppress the vortex shedding significantly and slightly increase in flutter

speed, compared with original section without fairing. In addition, those results shown that the modified section with fairing and soffit plates can significantly increase in flutter speed, compared with original section without fairing.

However, the interference effects occur when the two decks were located in parallel configurations with ratio between the gap distance of two decks and the width (x = 7.26/42.4 = 0.17, normalize with the width of new bridge). The Interferences effects of two-parallel bridge decks on vortex-induced vibration and flutter response can be summarized as follows.

(a) Bottom view of the two-sectional model

(b) Top view of the two-sectional model

Figure 7. Section model in wind tunnel.

(a) Aeroelastic rig support

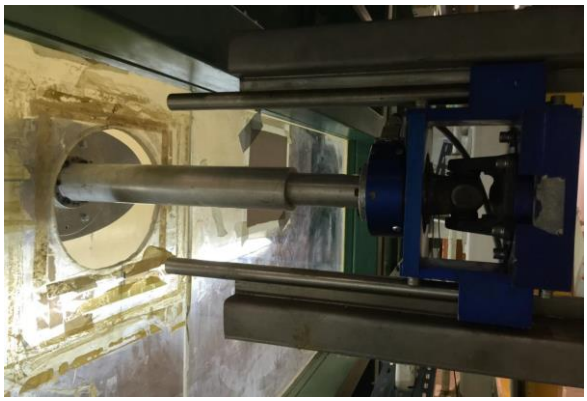

(b) Aerodynamic static rig support

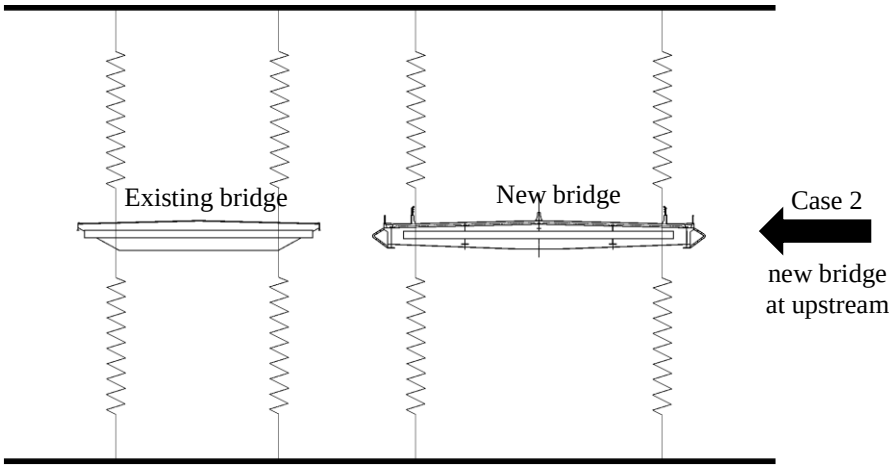

(c) Setup for aeroelastic test for two parallel bridges in wind tunnel

Figure 8. Setup of wind tunnel tests for two parallel bridges.

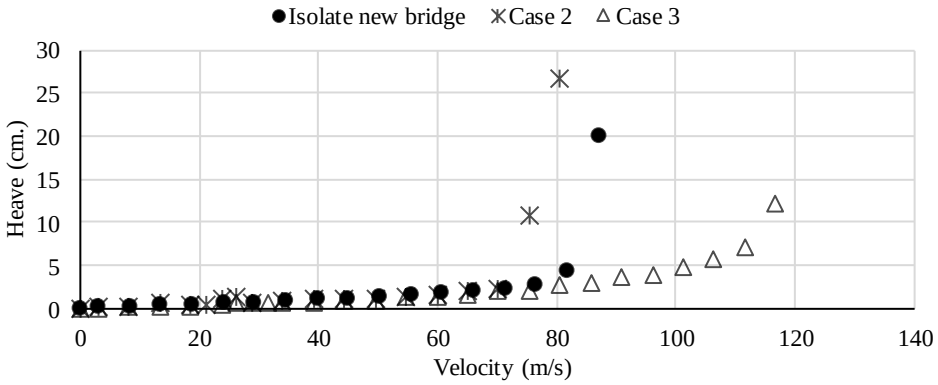

(a) Heave response

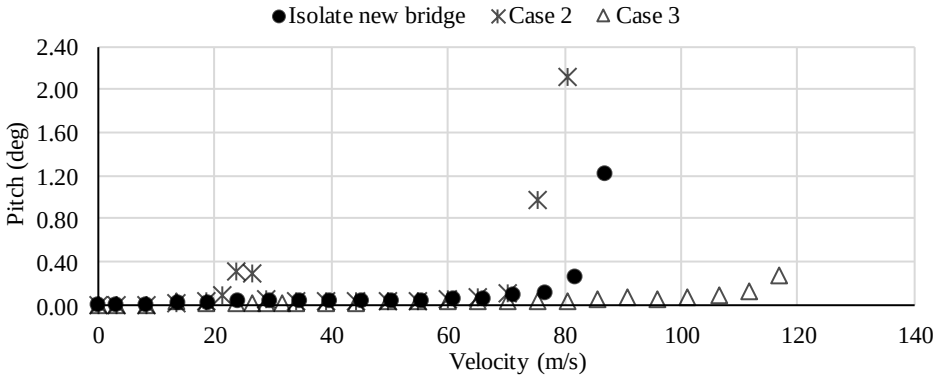

(b) Pitch response

Figure 9. RMS-V curve of new bridge in 3 configuration cases.

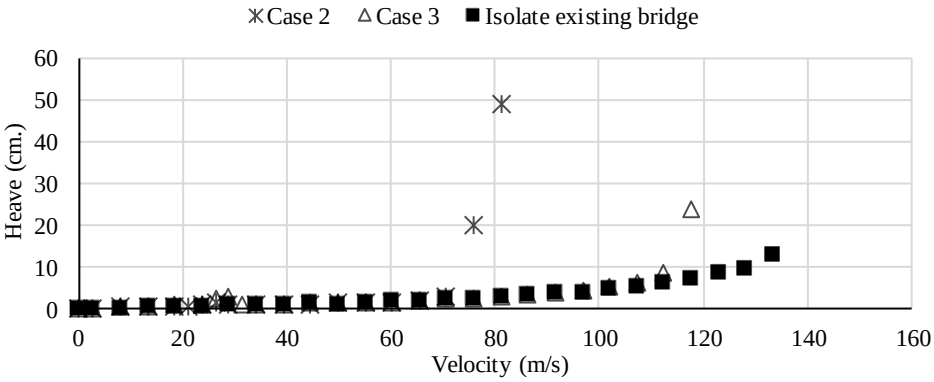

(a) Heave response

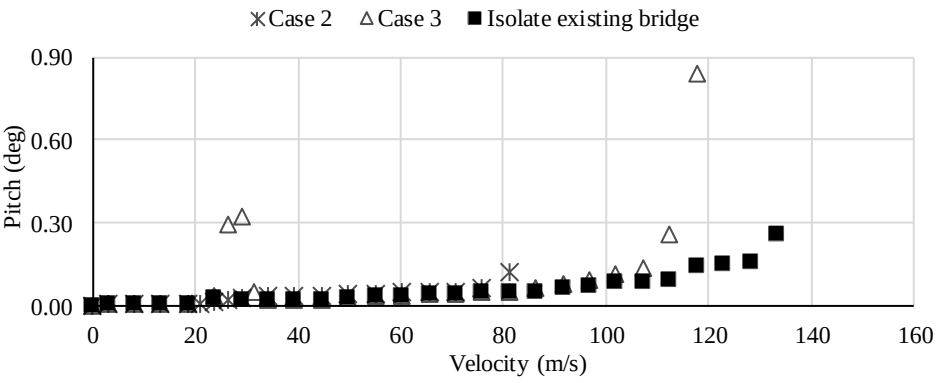

(b) Pitch response

Figure 10. RMS-V curve of existing bridge in 3 configuration case.

a) Vortex-induced vibration for the upstream new bridge and downstream existing bridge (Case 2)

Response of the new bridge and existing bridge are represented in term of RMS and velocity. Fig 9 show the RMS-velocity of new bridge and existing bridge in case 2. The Strouhal number (St) of new bridge in case 2 (new bridge located at upstream) was measured to be 3.021*0.043/1.924 = 0.067. The VIV occurs at mean wind speed of 23.63 m/s, this vortex-shedding speed is relatively high. The vortex-shedding excitation was also shown in torsional motion of new bridge. The maximum RMS vertical value of new bridge was 1.1 cm., this value is significantly lower than that of the 9.8 cm. allowable limit of vibration recommended in the wind-resistant design manual for highway bridges in Japan [13] but the maximum RMS torsional value of new bridge was 0.32°, this value is slightly higher than that of the 0.25° allowable limit of vibration recommended in the wind-resistant design manual for highway bridges in Japan (Sato, 2003).

The new bridge showed the large amplitude in torsional motion. The large amplitude in torsional motion of new bridge effected to heave and torsional motion of existing bridge. Therefore, the torsional frequency of 3.021 Hz of new bridge at mean speed of 23.63 m/s also appears in the existing bridge. The interference from new bridge affected to RMS vertical value of existing bridge was 1.09 cm. and RMS torsional value of existing bridge was 0.01°, these two values are significantly lower than those of the allowable limits of vibration recommended in the wind-resistant design manual for highway bridges in Japan [13].

b) Vortex induced vibration for the downstream new bridge and the upstream existing bridge (Case 3)

Fig. 10 show the RMS-velocity of new bridge and existing bridge in case 3, The VIV occurs at mean wind speed of 29.08 m/s, this vortex-shedding speed is relatively high. The vortex-shedding excitation was also shown in both vertical bending and torsional motion of existing bridge, which is located at upstream. The maximum RMS vertical value of existing bridge was 2.92 cm., this value is significantly lower than that of the 8.9 cm allowable limit of vibration recommended in the wind-resistant design manual for highway bridges in Japan [13] but the maximum RMS torsional value of new bridge was 0.31°, this value is slightly higher than that of the 0.17° allowable limit of vibration recommended in the wind-resistant design manual for highway bridges in Japan [13].

The existing bridge showed the large amplitude in torsional motion. The large amplitude in torsional motion of existing bridge effected to heave and torsional motion of new bridge. Therefore, the torsional frequency of 4.936 Hz. of existing bridge at mean wind speed of 29.08 m/s also appears in the new bridge. The interference from existing bridge affected to RMS vertical value of new bridge was 0.74 cm. and RMS torsional value of existing bridge was 0.023°, these two values are significantly lower than those of the allowable limits of vibration recommended in the wind-resistant design manual for highway bridges in Japan [13].

c) Comparison of the flutter response of new bridge from 3 configuration

Fig. 9 comparison the RMS-velocity (RMS-V) curve of new bridge from 3 cases. From the sectional bridge model test in wind tunnel under smooth winds, the response of new bridge from 3 configuration cased can be summarized as follows.

For the new bridge alone (case 1), the very abrupt transition with increasing velocity from the effectively zero torsional response amplitude to the clear instability occurs in the near neighborhood of mean wind speed of 81.84 m/s and completely flutter instability at mean wind speed of 87.09 m/s in prototype. The abrupt change in the vertical response at high wind speed is due to the effect of cross derivative H_2^* and H_3^*, which cause coupling of the torsional responses with the vertical response in term of damping and stiffness respectively [14]. It was found that the instability of the studied bridge model is the torsional flutter type. Since the studied bridge is the hard type flutter, the flutter instability has been defined as the mean wind speed at which this abrupt transition of torsional response was beginning in wind tunnel test or zero value of torsional damping ratio of the sectional model system. The stability limit is significantly high compared to the design wind speed.

For the new bridge located upstream and the existing bridge located downstream (case 2), the very abrupt transition with increasing velocity from the effectively zero torsional response amplitude to the clear instability occurs in the near neighborhood of mean wind speed of 70.18 m/s and completely flutter instability at mean wind speed of 75.35 m/s in prototype. It was found that the instability of the new bridge model is the torsional flutter type. The torsional spectral density of new bridge shows a huge alternating flutter. In this condition, the downstream existing bridge was subjected to galloping oscillations induced by the turbulent wake of upstream new bridge and it will be explained more detail in sub-section d). It should be noted that cases 2 result in significantly lower the flutter speed than cases 1.

When new bridge located downstream (case 3), the clear instability occurs in the near neighborhood of mean wind speed of 111.55 m/s and completely flutter instability at mean wind speed of 116.73 m/s in prototype. In cases 3, the new bridge shown the highest flutter speed from 3 configuration because the flutter speed of isolate existing bridge is significantly higher that of isolate new bridge (see Fig.10). The flutter instability of the new bridge reported that the similar torsional flutter type as case 1 and 2. The stability limit is extremely high compared to the design wind speed.

d) Comparison of the flutter response of existing bridge from 3 configuration cases

Fig. 10 comparison the RMS-velocity (RMS-V) curve of existing bridge from 3 cases. From the sectional bridge model test in wind tunnel under smooth winds, the response of existing bridge from 3 configuration cased can be summarized as follows.

For the existing bridge alone, the very abrupt transition with increasing velocity from the effectively zero torsional response amplitude to the clear instability occurs in the near neighborhood of mean wind speed of 128.29 m/s and completely flutter instability at mean wind speed of 133.51 m/s in prototype. It was found that the instability of the studied bridge model is the torsional flutter type. The stability limit is significantly high compared to the design wind speed.

For the existing bridge located upstream and the new bridge located downstream (case 3), the very abrupt transition with increasing velocity from the effectively zero torsional response amplitude to the clear instability occurs in the near neighborhood of mean wind speed of 111.55 m/s and completely flutter instability at mean wind speed of 116.73 m/s in prototype. It was found that the flutter instability of the existing bridge is the torsional flutter type. The torsional spectral density of existing bridge shows a huge alternating flutter. The torsional frequency of upstream existing bridge 4.547 Hz induced downstream new bridge and resulted in torsional flutter of downstream new bridge. It should be noted that unlike case 3 of new bridge, case 3 of existing bridge result in significantly lower the flutter speed than the isolate existing bridge because of the interference effects of two bridges.

(a)

(b)

(c)

Figure 11. (a) Overall wind load study of Bangkok Observation Tower in Bangkok, Thailand, by wind tunnel test; (b) high-frequency force balance model; (c) pressure measurement model.

When existing bridge located downstream (case 2), the clear instability occurs in the near neighborhood of mean wind speed of 70.18 m/s and completely flutter instability at mean wind speed of 75.35 m/s in prototype. The torsional response of new bridge with torsional frequency of 2.892 Hz generated turbulent wakes flow and resulted in H_1^* of existing bridge becomes zero at the reduced wind velocity ($U/n_h B$) of 6.82 corresponding to wind speed of 72.01 m/s (U =6.82*0.32*33 =72.01 m/s). This flutter speed agrees well with RMS-V curve of existing bridge in Fig. 10. In this case, the existing bridge shown the lowest flutter speed from 3 configuration. It can clearly see in H_1^* of existing bridge that the downstream existing bridge was subjected to galloping oscillation induced by the turbulent wake of upstream new bridge. The galloping oscillation of the existing bridge only in case 2 but not via versus in case 3 are caused by the shape and size of the upstream new bridge. The new bridge has the open deck (see Figs. 5 and 7) and much wider deck than the existing deck (see Fig. 7).

RESEARCH ON OVERALL WIND LOAD AND RESPONSE AND PRESSURE STUDY OF HISE-RISE BUILDINGS

The Bangkok Observation Tower

Wind load study for pressure measurement, overall wind load and response, and wind environment of Bangkok Observation Tower [15] were performed by TU-AIT wind tunnel test as shown in Figure 11. The Bangkok Observation Tower project is developed on Charoen Nakhon Road adjacent to the Chao Phraya River in Center Bangkok. The height at the crown is 459 m with diameter of 38 m at the bottom, 25 m at 300 m and 38 m at 380 m. The internal solid reinforced concrete core has a diameter of 19.10 m from ground level to 400 m. The outer perimeter makes of the steel composite diagrid. The height at the observation floor is 366 m.

(a)

(b)

(c)

Figure 12. (a) Overall wind load study of 548 Ploenchit building in Bangkok, Thailand, by wind tunnel test; (b) high-frequency force balance model; (c) pressure measurement model.

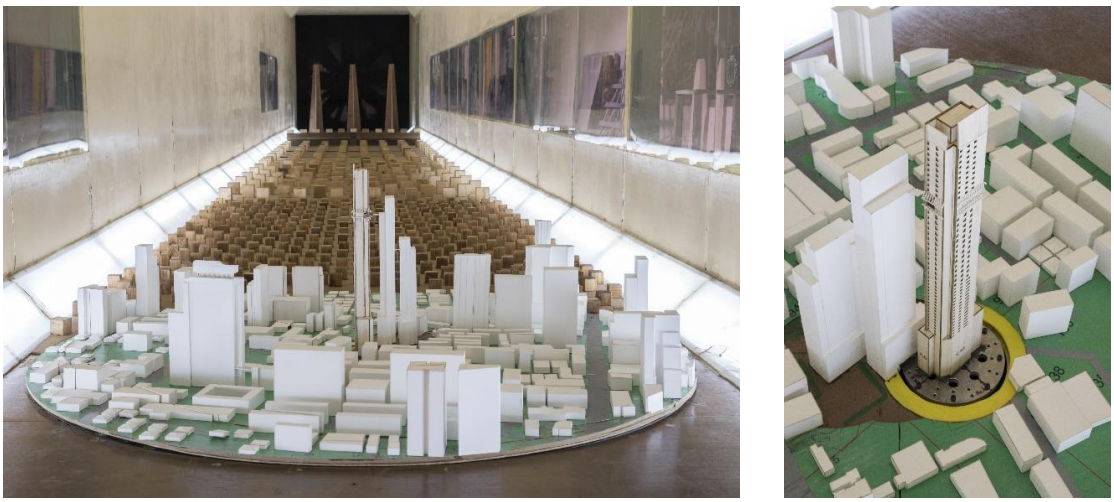

Figure 13. Overall wind load study of Park Thonglor in Bangkok, Thailand, by wind tunnel test and high-frequency force balance model.

(a)

(b)

(c)

Figure 14. (a) Overall wind load study of Noble Thonglor building in Bangkok, Thailand, by wind tunnel test; (b) high-frequency force balance model; (c) pressure measurement model.

The 548 Ploenchit Building

Wind load study for pressure measurement, overall wind load and response, and wind environment of 548 Ploenchit [16] were performed by TU-AIT wind tunnel test as shown in Figure 12. The 548 Ploenchit Building is the high-rise tower developed on Ploenchit Road in central Bangkok. The tower has 52 stories and 263.25 m equivalent roof high, 44.42 m equivalent width and 48 m equivalent depth.

The Park Thonglor Building

Wind load study for overall wind load and response of The Park Thonglor Building Project [17] were performed by TU-AIT wind tunnel test as shown in Figure 13. The Project is developed on Thonglor Road in central Bangkok. The project comprises 3 high-rise condominium towers. Three towers are connected by the moveable bridges at the top of towers. The tower A has 39 stories and 141.60 m roof high, 18.44 m equivalent width and 36.12 m equivalent depth. The tower B has 53 stories and 189.20 m roof high, 18.64 m equivalent width and 37.26 m equivalent depth. The tower C has 59 stories and 231.80 m roof high, 18.82 m equivalent width and 30.70 m equivalent depth.

The Noble Thonglor Building

Wind load study for pressure measurement, overall wind load and response, and wind environment of the Noble Thonglor [18] were performed by TU-AIT wind tunnel test as shown in Figures 14 and 15. The Noble Thonglor project is the high-rise buildings. The project is developed on Sukhumvit 55 Road in Bangkok. The Noble Thonglor has 48 stories and 207.55 m roof high, 28.71 m equivalent width and 29.12 m equivalent depth.

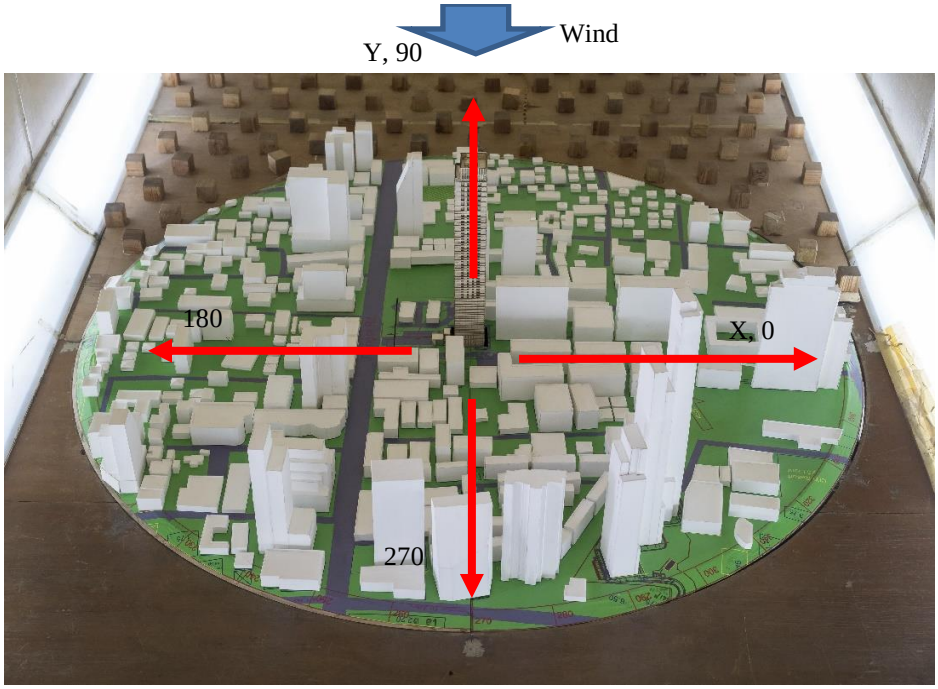

Figure 15. Wind directions and coordinate system of the Noble Thonglor building in wind tunnel.

Table 3. Comparisons of the expected peak base moments and torques from all wind-direction for three sets of dynamic properties, and two values of damping ratios.

Natural Frequency	Damping (ξ)	M_y (MN-m)		M_x (MN-m)		M_z (MN-m)	
		Peak	Deg.	Peak	Deg.	Peak	Deg.
0.80 f_o	0.020	-1,803	270	2,350	180	20	10
	0.010	-2,528	270	3,297	180	24	0
f_o	0.020	-1,401	260	-1,415	0	19	10
	0.010	-1,947	260	-1,957	0	24	0
1.2 f_o	0.020	-1,098	90	-1,091	0	-19	160
	0.010	-1,512	90	-1,486	0	24	0

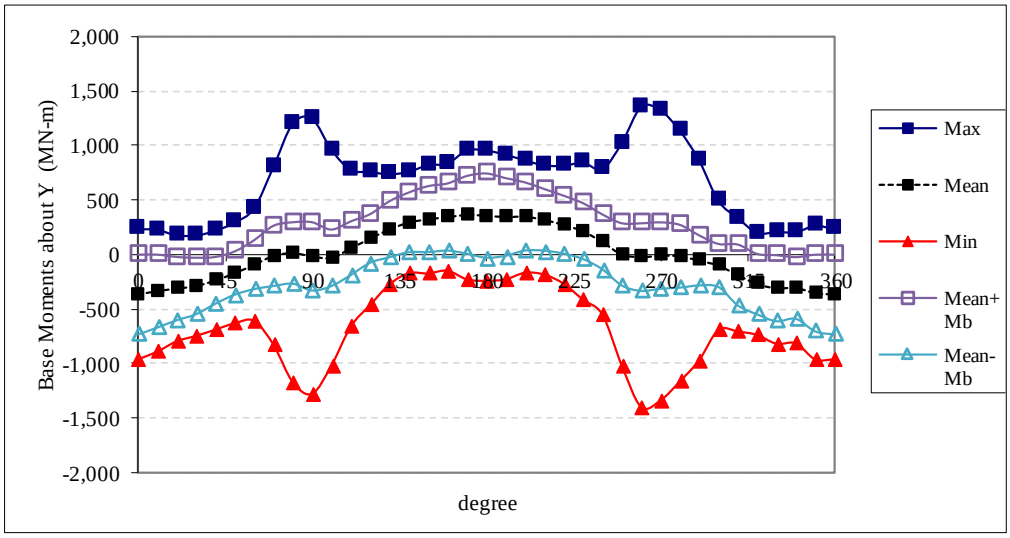

Figure 16. Expected peak base moments about Y-axis (Bending in X-direction) (Natural frequency f_o, damping ratio ξ = 0.02).

Table 4. Comparisons of the predicted peak accelerations from all wind-direction for three sets of dynamic properties, and two values of damping ratios.

Natural Freq.	Wind Speed	Damping (ξ)	Total acc, (mg)	
			Peak	Deg.
0.8 f_o	V_{10}	0.01	28.55	260
	V_{10}	0.005	40.38	260
	0.85 V_{10}	0.01	16.47	0
	0.85 V_{10}	0.005	23.29	0
f_o	V_{10}	0.01	21.54	0
	V_{10}	0.005	30.46	0
	0.85 V_{10}	0.01	13.15	260
	0.85 V_{10}	0.005	18.60	260
1.2 f_o	V_{10}	0.01	18.10	0
	V_{10}	0.005	25.60	0
	0.85 V_{10}	0.01	10.61	260
	0.85 V_{10}	0.005	15.00	260

a) For strength consideration of the Noble Thonglor building

For strength consideration with three natural frequencies (0.8f_o, f_o, 1.2f_o), two damping ratio ξ (0.02, 0.01), and V_{50}, the results are shown in Figures 15 and 16 and in Table 3 and can be summarized as follows.

For natural frequency f_o, and damping ratio = 0.020, the peak base moments M_x of -1,415 MN-m, M_y of -1,401 MN-m and torque M_z of 19 MN-m occur at wind direction 0, 260, and 10 degree, respectively. It should be noted that the peak base moments M_x and My are caused by the acrosswind load.

For studied building, the peak base moments are significantly reduced when building natural frequencies are increased from 1.0f_o to 1.2f_o. In contrast, the peak base moments are significantly increased when building natural frequencies are reduced from f_o to 0.80f_o.

b) For serviceability consideration of the Noble Thonglor building

For serviceability consideration, three natural frequencies (0.8f_o, f_o, and 1.2f_o), two damping ratios ξ (0.010 and 0.005), and two wind speeds (V_{10} and 0.85V_{10}), the results are shown in Table 4 and in Figures 15, 17 and 18 and can be summarized as follows.

For studied building, the peak accelerations are significantly reduced when damping ratio is increased from 0.005) to (0.010 This is because the peak acceleration responses are mainly caused by the resonant parts of acrosswind and alongwind loads.

For studied building, the peak accelerations are moderately reduced when building natural frequencies are increased

from f_o to 1.2f_o. In contrast, the peak accelerations are moderately increased when building natural frequencies are reduced from f_o to 0.8f_o.

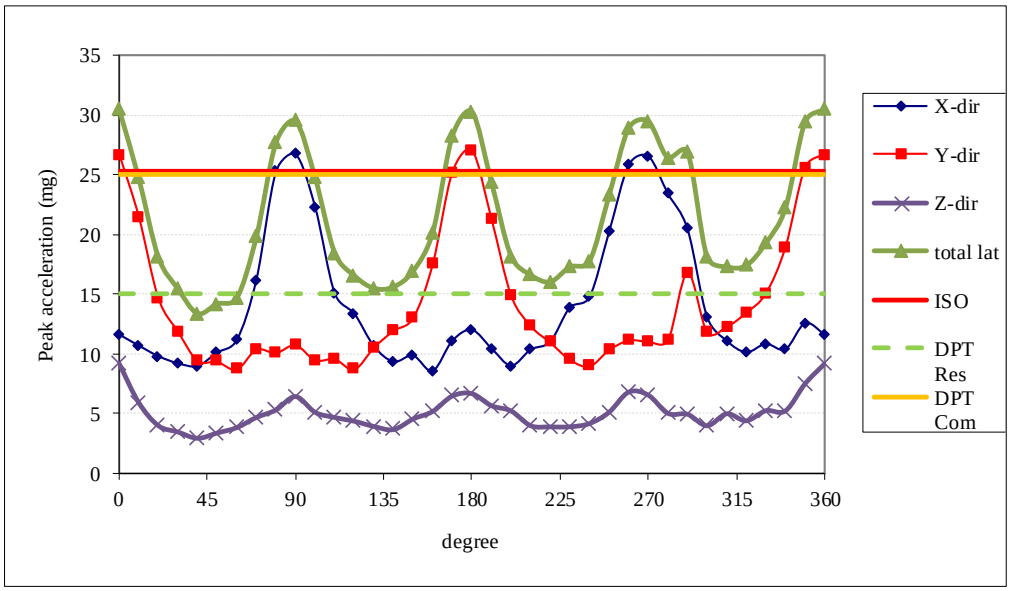

Figure 17. Predicted peak acceleration responses (Natural frequency f_0, damping ratio ξ = 0.005 and V_{10}).

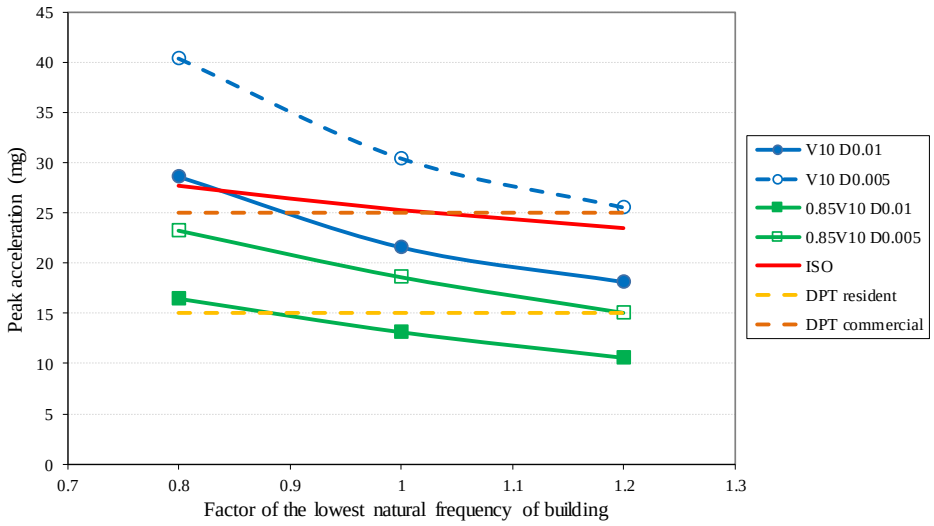

Figure 18. Comparisons of the predicted peak acceleration responses and the recommended serviceability design for human comfort criteria for three sets of dynamic properties (0.8f_o, f_o, and 1.2f_o) and two values of damping ratios (0.005 and 0.01).

CONCLUSION

The new development of wind loading standard for building design in Thailand includes the specified wind load and response, reference wind speed map, natural frequency and damping of building, table for design wind loads for main structures, secondary members and claddings for low-rise buildings, wind tunnel test procedure, commentary, numerical examples, computer program for calculation of wind load and response, and wind load on miscellaneous structures.

The research on wind effects on long-span brifges showed that the interference effects of two bridges decks on aerodynamic coefficients result in the slightly reduction of the drag coefficient compared with the new bridge alone. The two parallel configurations of the bridge result in vortex-induced vibrations and significantly lower the flutter speed compared with the new bridge alone. The huge torsional motion from upstream new bridge (case 2) generated turbulent wakes flow and resulted in vertical aerodynamic damping H1* of existing bridge becomes zero at wind speed of 72.01 m/s. In this case, the downstream existing bridge was subjected to galloping oscillation induced by the turbulent wake of upstream new bridge. The new bridge also results in significant reduction of the flutter speed of existing bridge from the 128.29 m/s flutter speed of the isolated existing bridge to the 75.35 m/s flutter speed of downstream existing bridge.

For the flexible and high-rise buildings, the peak base moments and the peak accelerations are caused by the across-wind load.

Since the new development of DPT standard 1311-50, wind load standard and wind load studies of buildings and bridges by TU-AIT wind tunnel test have been increasingly interesting to Thai engineers.

ACKNOWLEDGEMENT

The new development of wind loading standard for building design in Thailand is financially supported by Department of Public Works and Town & Country Planning and the first author is the project head. The authors wish to express their sincere appreciations to Epsilon Co. Ltd. in Association with Wiecon Co. Ltd., and Expressway Authority of Thailand for their financial supports in wind tunnel test for the two parallel cable-stayed bridges. The authors are also greatly indebted to the many clients listed in the references for their interests in using TU-AIT wind tunnel.

REFERENCES

[1] P. Lukkunaprasit, P. Pheinsusom, and N. Euasiriwam, Wind Loading for Tall Building Design in Thailand, *Proc. of 2nd National Convention on Civil Engineering*, Chiangmai, Thailand, pp. 51-61(in Thai), 1995.

[2] V. Boonyapinyo, Comparison between Wind and Earthquake Loads for High-Rise Building Design in Thailand, *Proc. of International Seminar on Earthquake Resistant Design of Structures*, Chiangmai, Thailand., pp. 416-432 (in Thai), 1998.

[3] Engineering Institute of Thailand, E.I.T. Standard 1018-46, Wind Loading Code for Building Design (in Thai), 2003.

[4] National Building Code of Canada, issued by the Canadian Commission on Building and Fire Codes, *National Research Council of Canada*, Ottawa, Canada, 1995.

[5] V. Boonyapinyo, P. Lukkunaprasit, S, Chucheepsakul, P. Warnitchai, N. Poovarodom, S. Thepmongkorn., N. Limsamphancharoen., and S. Leelataviwat, Wind Loading for Building Design in Thailand, Final Report for DPT 1311-50 Standard (2007), Submitted to Department of Public Works and Town & Country Planning (in Thai), 2007.

[6] DPT Standard, DPT 1311-50: Wind Loading Calculation and Response of Buildings, *Department of Public Works and Town & Country Planning* (in Thai), 2007.

[7] National Building Code of Canada, issued by the Canadian Commission on Building and Fire Codes, *National Research Council of Canada*, Ottawa, Canada, 2005.

[8] AIJ, Recommendation for Loads on Buildings, *Architectural Institute of Japan*, 2004.

[9] ASCE Standard, ASCE7-05: Minimum Design Loads for Buildings and Other Structures, *American Society of Civil Engineers*, New York, 2005.

[10] AES Group, Kinematics and OPAC, The Rama IX Bridge Tenth-Year Inspection, Submitted to Expressway and Rapid Transit Authority of Thailand, 2001.

[11] Epsilon Co. Ltd. and Weicon Co. Ltd., EXAT Bridge Project: Mode Shape of Structure second issue, Thailand, 2016.

[12] V. Boonyapinyo, T. Janesupasaeree. and W. Thamasungkeeti, "Identification of flutter derivatives of bridge decks by stochastic subspace method", *The Seventh Asia-Pacific Conference on Wind Engineering*, Taipei, Taiwan, November, 2009.

[13] H. Sato, "Wind-resistant design manual for highway bridges in Japan", *J. Wind Eng. Ind. Aerodyn.*, Vol. 91, pp. 1499-1509, 2003. https://doi.org/10.1016/j.jweia.2003.09.012

[14] V. Boonyapinyo, T. Miyata, and H. Yamada, "Advanced aerodynamic analysis of suspension bridges by state-space approach.", *J.Struct.Eng.*, Vol. 125(12), pp. 1357–1366, 1999.

[15] V. Boonyapinyo, M. Magteppong, J. Junruang, and B. Bhadrakom, Wind Load Study for Bangkok Observation Tower Project by Wind Tunnel Test, Final Report, Thammasat University Research and Consultancy Institute (TU-RAC), Submitted to Bangkok Sky Tower Foundation, 2017.

[16] V. Boonyapinyo, and J. Junruang, Wind Load Study for 548 Ploenchit Buildingr Project by Wind Tunnel Test, Final Report, Thammasat University Research and Consultancy Institute (TU-RAC), Submitted to RML 548 Co., Ltd. and Meinhardt (Thailand) Co., Ltd., 2018.

[17] V. Boonyapinyo, and J. Junruang, Wind Load Study for Park Thonglor Buildingr Project by Wind Tunnel Test, Final Report, Thammasat University Research and Consultancy Institute (TU-RAC), Submitted to Origin Park T1 Co., Ltd., Umbau Co.,Ltd., and Infra Technology Service Co., Ltd.., 2021.

[18] V. Boonyapinyo, J. Junruang, and S. Supabphol, Wind Load Study for Noble Thonglor Buildingr Project by Wind Tunnel Test, Final Report, Thammasat University Research and Consultancy Institute (TU-RAC), Submitted to Noble Development Public Co., Ltd. and Stonehenge Co,. Ltd.., 2020.